

Optical properties of pulsed laser deposited rutile titanium dioxide films on quartz substrates determined by Raman scattering and transmittance spectra

Z. G. Hu, W. W. Li, J. D. Wu, J. Sun, Q. W. Shu, X. X. Zhong, Z. Q. Zhu, and J. H. Chu

Citation: [Applied Physics Letters](#) **93**, 181910 (2008); doi: 10.1063/1.3021074

View online: <http://dx.doi.org/10.1063/1.3021074>

View Table of Contents: <http://scitation.aip.org/content/aip/journal/apl/93/18?ver=pdfcov>

Published by the [AIP Publishing](#)

Articles you may be interested in

[Influence of plasma density on the chemical composition and structural properties of pulsed laser deposited TiAlN thin films](#)

[Phys. Plasmas](#) **21**, 053509 (2014); 10.1063/1.4879025

[Substrate influence on the optical and structural properties of pulsed laser deposited BiFeO₃ epitaxial films](#)

[J. Appl. Phys.](#) **107**, 123524 (2010); 10.1063/1.3437059

[Structural and optical properties of thin lead oxide films produced by reactive direct current magnetron sputtering](#)

[J. Vac. Sci. Technol. A](#) **19**, 2870 (2001); 10.1116/1.1410948

[Spectroscopic ellipsometry and Raman study of fluorinated nanocrystalline carbon thin films](#)

[J. Appl. Phys.](#) **90**, 813 (2001); 10.1063/1.1378337

[Influence of ion-beam energy and substrate temperature on the synthesis of carbon nitride thin films by nitrogen-ion-assisted pulsed laser deposition](#)

[J. Appl. Phys.](#) **86**, 4954 (1999); 10.1063/1.371465



Optical properties of pulsed laser deposited rutile titanium dioxide films on quartz substrates determined by Raman scattering and transmittance spectra

Z. G. Hu,^{1,a)} W. W. Li,¹ J. D. Wu,² J. Sun,² Q. W. Shu,³ X. X. Zhong,^{3,b)} Z. Q. Zhu,¹ and J. H. Chu¹

¹Key Laboratory of Polar Materials and Devices, Ministry of Education, East China Normal University, Shanghai 200241, People's Republic of China

²State Key Laboratory for Advanced Photonic Materials and Devices, Department of Optical Science and Engineering, Fudan University, Shanghai 200433, People's Republic of China

³Department of Physics, Shanghai Jiao Tong University, Shanghai 200240, People's Republic of China

(Received 1 September 2008; accepted 20 October 2008; published online 6 November 2008)

Optical response of rutile TiO₂ films grown under different laser energy by pulsed laser deposition has been investigated by Raman scattering and spectral transmittance. Dielectric functions in the photon energy range of 1.24–6.5 eV have been extracted by fitting the experimental data with the Adachi's model [S. Adachi, Phys. Rev. B **35**, 7454 (1987)]. The refractive index dispersion in the transparent region is mainly ascribed to the higher A₁-A₂ electronic transitions for the rutile TiO₂ films. Owing to slightly different crystalline structures and film densities, the optical band gap linearly increases with increasing packing density. The phenomena were confirmed by different theoretical evaluation methods. © 2008 American Institute of Physics. [DOI: 10.1063/1.3021074]

For several decades, much effort has been made on the studies of wide band gap transition metal (TM) oxide materials with regard to electrical, optical, chemical, and magnetic properties.^{1,2} Recently, titanium dioxide (TiO₂) has received much attention in view of their wide applications in chemical sensing and catalysis, nonlinear optics, optoelectronic devices, and so on.^{3,4} As we know, TiO₂ has three distinct crystalline structures, rutile, anatase, and brookite, which can be expected to exhibit different physical and chemical properties.⁵ In particular, the rutile phase structure has been considered to be most suitable for optoelectronics applications due to its high dielectric constants and optical constants.^{6,7} Although there are some reports on optical and electrical properties of TiO₂ material,^{8–10} few results about optical properties of rutile TiO₂ bulk crystal have been presented up to now.^{11,12} It should be noted that the values from rutile TiO₂ films have been reported only limited to the transparent region (i.e., visible range).¹³ It is well known that films can be deposited directly on diversified substrates and are expected to yield better sensitivity and faster response than the equivalent bulk single crystal. Therefore, a detailed dielectric function study above the optical band gap (OBG) is still necessary to exploit its optoelectronic applications of the oxide films with the rutile phase.

There has been an increased interest in TiO₂-based diluted magnetic oxides (DMO), which was amplified by theoretical predictions suggesting that ferromagnetism of diluted magnetic compounds with Curie temperatures above room temperature (RT) could be obtained.^{14–16} For example, both cobalt-doped and undoped TiO₂ films experimentally show the remarkable RT ferromagnetism, which suggests that the contributions from the TM element to the physical properties of the host lattice matrix are unclear and require further investigations.^{16,17} It can be expected that given the complex phase diagram of oxides, studies of the undoped

and stoichiometric compounds could give a fundamental insight into the physics governing the doped version of these DMO. It is desirable to carry out a delicate study regarding these essential properties of rutile TiO₂ material.¹⁶ In this letter, the optical properties of rutile TiO₂ layers grown at different laser energy are studied in detail.

Rutile TiO₂ films were grown by electron cyclotron resonance plasma-assisted pulsed laser deposition technique.¹⁸ Double-side polished quartz wafers, which were selected for the ultraviolet transmittance measurements and silicon (Si) wafers, were used as the substrates. The laser used is a frequency-doubled neodymium-doped yttrium aluminum garnet laser at a repetition rate of 10 Hz. The laser energy per pulse on target surface was varied at 30, 50, 60, 70, and 80 mJ, respectively. The crystalline structure of the TiO₂ films on Si substrates was analyzed by x-ray diffraction (XRD) using Cu K α radiation. There are the diffraction peaks (110), (101), and (211), and no impurity phases observed, which confirm that the films are of the rutile phase (not shown). According to Scherrer's equation, the average grain size is about 30 nm and remains nearly unchanged with the laser energy. Raman scattering experiments were done by a Jobin-Yvon LabRAM HR 800UV micro-Raman spectrometer. A He–Cd laser with the wavelength of 325 nm (3.82 eV) was applied as the excited light. Figure 1 shows the lattice vibrations of rutile TiO₂ layers grown at different laser energy. It further indicates that all five samples have the pure rutile structure. The E_g and A_{1g} phonon modes are located at 415 and 610 cm⁻¹, respectively. Note that these values slightly deviate from the bulk data (418 and 612 cm⁻¹, respectively).⁷ This could be ascribed to different crystalline structures and stresses between the film and substrate due to the diverse thickness. In addition, a broadening band near 830 cm⁻¹ can be assigned to the B_{2g} mode.² The optical transmittance at RT was recorded with a double beam ultraviolet-infrared spectrophotometer (PerkinElmer Lambda 950) at the photon energy from 1.24 to 6.5 eV (190–1000 nm) with a spectral resolution of 2 nm.

^{a)}Electronic mail: zghu@ee.ecnu.edu.cn.

^{b)}Electronic mail: xxzhong@sjtu.edu.cn.

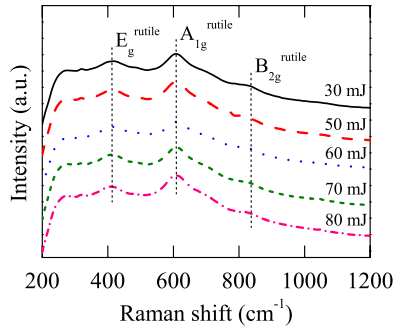


FIG. 1. (Color online) Raman scattering of rutile TiO₂ films grown on quartz substrates at different laser energies with the excitation line of 325 nm. The dashed lines clearly indicate the lattice vibration modes from the rutile phase.

A three-phase layered structure (air/film/substrate) was used to calculate the transmittance spectra of the TiO₂ films.^{19,20} For wide band gap semiconductor materials, the dielectric response, which can be described by the contribution from the lowest three-dimensional M_0 type critical point (CP), is written as the following Adachi's²¹ model: $\bar{\epsilon}(E) = \epsilon_\infty + \{A_0[2 - (1 + \chi_0)^{1/2} - (1 - \chi_0)^{1/2}]\} / (E_g^{3/2} \chi_0^2)$. Here, $\chi_0 = (E + i\Gamma)/E_g$, ϵ_∞ is the high-frequency dielectric constant, E_g is the fundamental optical transition energy, E is the incident photon energy, and A_0 and Γ are the strength and broadening parameters of the E_g transition, respectively. The experimental transmittance spectra of rutile TiO₂ films are shown in Fig. 2 with the dotted lines. The transmittance spectra are similar to those reported by Ting *et al.*¹³ Note that the interference oscillation period is similar from the film samples, except for sample D grown at the laser energy of 70 mJ. This is because the film has the maximum thickness. Moreover, its fundamental absorption edge becomes much sharper, as compared with other samples from the inset of Fig. 2. It indicates that there are Urbach tail states, which can be due to crystalline defects and grain boundary.²² The dielectric functions of the TiO₂ films can be uniquely determined by fitting the model function to the experimental data. The fitted parameter values and thicknesses are summarized in Table I, and the simulated transmittance data are also shown in Fig. 2 by the solid lines. A good agreement is obtained between the experimental and calculated spectra in the entirely measured

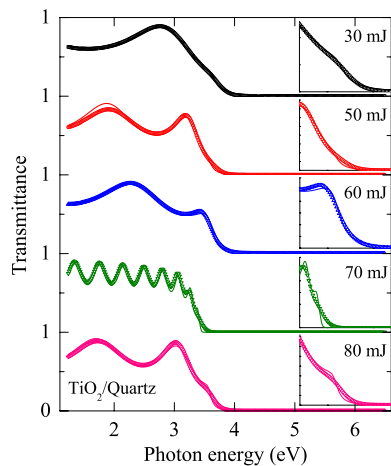


FIG. 2. (Color online) Experimental (dotted lines) and best-fit (solid lines) transmittance spectra of rutile TiO₂ films from the near-infrared to ultraviolet photon energy region. The insets show an enlarged fitting fundamental band gap region of 3.2–4.2 eV.

TABLE I. Adachi's (Ref. 21) parameter values of rutile TiO₂ films are determined from the simulation of transmittance spectra in Fig. 2. The 90% reliability of the fitting parameters is given in parentheses.

Samples	Energy (mJ)	Thickness d (nm)	ϵ_∞	A_0 (eV ^{3/2})	E_g (eV)	Γ (eV)
A	30	82 (0.2)	0.01 (0.13)	160 (3)	3.64 (0.01)	0.05 (0.01)
B	50	127 (1)	0.03 (0.20)	165 (4)	3.59 (0.01)	0.06 (0.01)
C	60	109 (1)	1.16 (0.15)	121 (3)	3.62 (0.01)	0.07 (0.01)
D	70	620 (6)	0.74 (0.11)	104 (3)	3.44 (0.01)	0.02 (0.01)
E	80	149 (1)	0.73 (0.24)	131 (6)	3.59 (0.01)	0.05 (0.01)

photon energy range, especially near the fundamental band gap region (see the insets of Fig. 2).

The evaluated dielectric functions of the rutile TiO₂ films are shown in Fig. 3. The evolution of $\bar{\epsilon}$ with the photon energy is a typical optical response behavior of dielectric and/or semiconductors.^{11,21} Generally, the real part ϵ_1 increases with the photon energy and approaches the maximum, then decreases with further increasing photon frequency due to the known Van Hove singularities.²¹ At the photon energy of 2.0 eV, the ϵ_1 value was approximately varied from 5.4 to 6.8 for the films grown at different laser energies. This suggests that the refractive index n correspondingly increases from 2.31 to 2.61 due to a smaller extinction coefficient κ (about 10^{-3}). These values are less than that from bulk crystal (2.75) (Ref. 13) and in good agreement with that reported in Ref. 12 (2.56). Note that there is a sharper feature in the ϵ_1 near the maximum, especially for the films deposited at the laser energy of 70 mJ, which has much smaller broadening value (about 0.02 eV). In the wide transparent region, the imaginary part ϵ_2 is down to zero. As the photon energy further increases, the ϵ_2 sharply increases to about 5 eV and slowly decreases up to the present measurement limitation (6.5 eV). It indicates that strong photon absorption appears, showing the interband transition behavior.

As we know, a different crystalline structure can result in the electronic band variation, which accordingly affects the optical and dielectric responses.^{5,23} It is well known that the n is related to the packing density (σ) and polarizability (P_m)

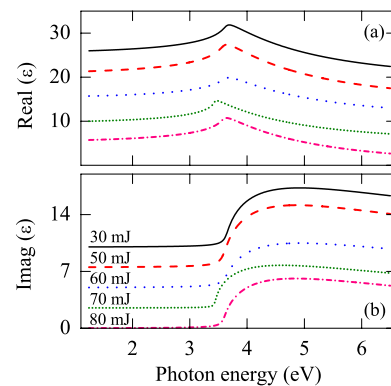


FIG. 3. (Color online) The dielectric function (a) real part and (b) imaginary part for rutile TiO₂ films grown at different laser energies in the photon energy range of 1.24–6.5 eV. For clarity, $\text{Re}(\epsilon)$ and $\text{Im}(\epsilon)$ parts are vertically shifted by adding 5 and 2.5, respectively.

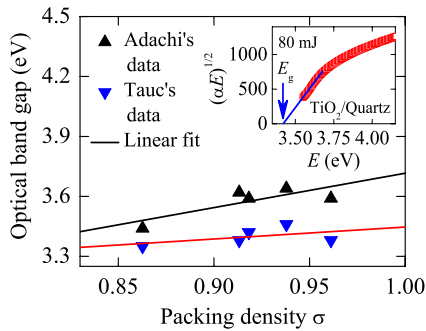


FIG. 4. (Color online) Film packing density effects on the OBG determined from Adachi's model (Ref. 21) and Tauc's theoretical calculation, respectively. The solid lines are the linearly fitting results to guide the eyes. Note that the inset shows the E_g determination of rutile TiO_2 film based on Tauc's formula.

of a given material by the following Lorentz-Lorentz relation: $(n^2-1)/(n^2+2) \propto C_A P_m \sigma m^{-1}$.¹⁰ Here, C_A is the Avogadro's constant and m is the molecular weight. Note that the formula $C_A P_m/m = (n_b^2-1)/(n_b^2+2)$ and n_b is the refractive index of the bulk crystal. Generally, the evaluated packing density with the aid of n at 2.0 eV decreases with increasing laser energy and is strikingly varied from 86% to 96% for TiO_2 films. The changed packing density suggests the partial crystalline structure distortion of rutile films, which provides the perturbation on the energy band structure and induces the optical response discrepancy. Therefore, the variation in the dielectric function (i.e., electronic structure) could be ascribed to changes in the packing density from the rutile films.

The OBG energy of the TiO_2 films corresponds to transitions between extended states in both valence and conduction bands, where the power law behavior of Tauc $(\alpha E)^{1/2} \propto (E - E_{g,\text{expt}})$ for allowed indirect transition, and $E_{g,\text{expt}}$ is the OBG energy.^{10,13} So the straight line between $(\alpha E)^{1/2}$ and E will provide the value of the $E_{g,\text{expt}}$, as seen in the inset of Fig. 4 for sample E. Note that the Adachi's²¹ model can also give the fundamental band gap (Table I). From the fitting parameters, the E_g is varied from 3.44 ± 0.01 to 3.64 ± 0.01 eV for different packing densities. However, the empirical Tauc's relationship presents a slightly smaller value from 3.42 to 3.46 eV. Nevertheless, both of them show a linearly increasing trend with increasing film packing density (see Fig. 4). Note that the OBG energy and σ of the film grown at 70 mJ are minimum due to a larger thickness. It should be emphasized that the present OBG data are considerably larger than those reported from the experimental and theoretical evaluations for the rutile phase structure.^{5,13,22,23} However, these values are in agreement with the results by Jellison Jr. *et al.*⁸ The peak width of the A_{1g} phonon mode is varied from 76.7 ± 1.8 to 87.1 ± 2.1 cm^{-1} for different packing densities, respectively. These values are larger than those of nanostructured rutile TiO_2 materials, which confirms that the average grain size is about several tens of nanometers.²⁴ This could be ascribed to the fact that the OBG energy strikingly increases with decreasing grain size (about 30 nm) and increasing packing density for the low-dimensional film structure owing to the known quantum confinement effect.²⁵

In rutile TiO_2 films, the electronic transitions are due to the crystal field and electrostatic interaction between O_{2p} ionic orbitals, which play an important role in the band structure.⁵ In particular, the conduction band comes mainly

from Ti_{3d} strongly hybridized with O_{2p} orbitals. Therefore, the crystal structure distortion could result in the OBG variation for different film packing densities. On the other hand, a broadening peak near 5.0 eV can be observed in the ϵ_2 spectra. Obviously, this is related to the higher CP virtual transitions (A_1-A_2), which are located between 4.0 and 5.4 eV and attributed to splitting in the $\text{O}_{2p_{xy}}$ orbitals.^{11,23} Nevertheless, the double-peak feature has not been observed due to the polycrystalline structure of the present rutile TiO_2 layers. It indicates that the optical dispersion in the transparent region is mainly ascribed to the higher A_1-A_2 electronic transitions and not to the fundamental band gap energy, which agrees with the theoretical expectation.^{5,23}

In summary, the laser energy dependence of the dielectric function in rutile TiO_2 films has been determined by the spectral transmittance technique. The OBG energy is about 3.5 eV and presents a linearly increasing trend with increasing film packing density.

This work was financially supported by Shanghai Pujiang Program (Contract No. 07PJ14034), Major State Basic Research Development Program of China (Contract No. 2007CB924901), and Shanghai Municipal Commission of Science and Technology Project (Contract Nos. 07JC14018, 07DZ22943, 08JC1409000, and 08520706100).

- ¹R. Asahi, T. Morikawa, T. Ohwaki, K. Aoki, and Y. Taga, *Science* **293**, 269 (2001).
- ²J. Zhang, M. J. Li, Z. C. Feng, J. Chen, and C. Li, *J. Phys. Chem. B* **110**, 927 (2006).
- ³J. E. Spanier, R. D. Robinson, F. Zhang, S. W. Chan, and I. P. Herman, *Phys. Rev. B* **64**, 245407 (2001).
- ⁴T. Mazza, E. Barborini, P. Piseri, P. Milani, D. Cattaneo, A. Li Bassi, C. E. Bottani, and C. Ducati, *Phys. Rev. B* **75**, 045416 (2007).
- ⁵S.-D. Mo and W. Y. Ching, *Phys. Rev. B* **51**, 13023 (1995).
- ⁶F. Zhang, Z. H. Zheng, X. Z. Ding, Y. J. Mao, Y. Chen, Z. Y. Zhou, S. Q. Yang, and X. H. Liu, *J. Vac. Sci. Technol. A* **15**, 1824 (1997).
- ⁷V. Swamy, C. B. Muddle, and Q. Dai, *Appl. Phys. Lett.* **89**, 163118 (2006).
- ⁸G. E. Jellison, Jr., L. A. Boatner, J. D. Budai, B.-S. Jeong, and D. P. Norton, *J. Appl. Phys.* **93**, 9537 (2003).
- ⁹J. Park, J.-Y. Lee, and J.-H. Cho, *J. Appl. Phys.* **100**, 113534 (2006).
- ¹⁰G. He, L. D. Zhang, G. H. Li, M. Liu, and X. J. Wang, *J. Phys. D* **41**, 045304 (2008).
- ¹¹M. Cardona and G. Harbeke, *Phys. Rev.* **137**, A1467 (1965).
- ¹²G. E. Jellison, Jr., F. A. Modine, and L. A. Boatner, *Opt. Lett.* **22**, 1808 (1997).
- ¹³C.-C. Ting, S.-Y. Chen, and D.-M. Liu, *J. Appl. Phys.* **88**, 4628 (2000).
- ¹⁴T. Dietl, H. Ohno, F. Matsukura, J. Cibert, and D. Ferrand, *Science* **287**, 1019 (2000).
- ¹⁵Y. Matsumoto, M. Murakami, T. Shono, T. Hasegawa, T. Fukumura, M. Kawasaki, P. Ahmet, T. Chikyow, S. Koshihara, and H. Koinuma, *Science* **291**, 854 (2001).
- ¹⁶T. Fukumura, H. Toyosaki, K. Ueno, M. Nakano, and M. Kawasaki, *N. J. Phys.* **10**, 055018 (2008).
- ¹⁷N. H. Hong, J. Sakai, N. Poirot, and V. Brizé, *Phys. Rev. B* **73**, 132404 (2006).
- ¹⁸D. Yu, Y. F. Lu, N. Xu, J. Sun, Z. F. Ying, and J. D. Wu, *J. Vac. Sci. Technol. A* **26**, 380 (2008).
- ¹⁹O. S. Heaven, *Optical Properties of Thin Solid Films* (Dover, New York, 1991), Chap. 4, p. 69.
- ²⁰Z. G. Hu, Y. W. Li, M. Zhu, Z. Q. Zhu, and J. H. Chu, *Appl. Phys. Lett.* **92**, 081904 (2008).
- ²¹S. Adachi, *Phys. Rev. B* **35**, 7454 (1987); **38**, 12345 (1988).
- ²²H. Tang, F. Levy, H. Berger, and P. E. Schmid, *Phys. Rev. B* **52**, 7771 (1995).
- ²³K. M. Glassford and J. R. Chelikowsky, *Phys. Rev. B* **46**, 1284 (1992).
- ²⁴V. Swamy, *Phys. Rev. B* **77**, 195414 (2008).
- ²⁵Z. G. Hu, Y. W. Li, M. Zhu, Z. Q. Zhu, and J. H. Chu, *Phys. Lett. A* **372**, 4521 (2008).